The crystal structure of khinite and polytypism in khinite and parakhinite

M. A. COOPER[1], F. C. HAWTHORNE[1],* AND M. E. BACK[2]

[1] Department of Geological Sciences, University of Manitoba, Winnipeg, Manitoba, Canada, R3T 2N2
[2] Department of Earth Sciences, Royal Ontario Museum, 100 Queen's Park, Toronto, Ontario, Canada, M5S 2C6

ABSTRACT

The crystal structure of khinite, $Pb^{2+}Cu_3^{2+}Te^{6+}O_6(OH)_2$, orthorhombic, a = 5.7491(10), b = 10.0176(14), c = 24.022(3) Å, V = 1383.6(4) Å^3, space group $Fdd2$, Z = 8, D_{calc} = 6.29 g/cm^3, from the Empire mine, Tombstone, Arizona, USA, has been solved by direct methods and refined to R_1 = 3.2% on the basis of 636 unique observed reflections. There is one distinct Te site occupied by Te and coordinated by six O atoms in an octahedral arrangement with a <Te−O> distance of 1.962 Å, typical of Te^{6+}. There are three octahedrally-coordinated Cu sites, each of which is occupied by Cu^{2+} with <Cu−O> distances of 2.132, 2.151 and 2.308 Å, respectively. Each Cu octahedron shows four short meridional bonds (~1.95 Å) and two long apical bonds (2.46−2.99 Å) characteristic of Jahn-Teller-distorted Cu^{2+} octahedra. There is one distinct Pb site occupied by Pb and coordinated by six O atoms and two (OH) groups with a <Pb−O, OH> distance of 2.690 Å. TeF_6 and $CuΦ_6$ octahedra share edges and corners to form an [$MΦ_2$] (where Φ = O, OH) layer of composition [$TeCu_3Φ_8$]. These layers stack along the c axis at 6 Å intervals with Pb atoms between the layers. Identical layers occur in the structure of parakhinite, $Pb^{2+}Cu_3^{2+}Te^{6+}O_6(OH)_2$, hexagonal, a = 5.765(2), c = 18.001(9) Å, V = 518.0(4) Å^3, space group $P3_2$, Z = 3, D_{calc} = 6.30 g/cm^3. It is only the relative stacking of the $TeCu_3Φ_8$ layers in the c direction that distinguishes the two structures, and hence khinite and parakhinite are polytypes.

Introduction

KHINITE is a Pb-Cu tellurate discovered on the dumps of the Old Guard mine in Tombstone, Arizona, USA and described by Williams (1978). It is a rare secondary mineral associated with parakhinite, dugganite, quetzalcoatlite, tlapallite, tenorite, chlorargyrite, chrysocolla, gold and quartz, and occurs as deep-green crystals that can be replaced by dugganite. The khinite here formed by oxidation of gold-telluride ores in highly-acidic minewaters. The crystal structure of parakhinite was reported by Burns *et al.* (1995),

and the chemical formula of parakhinite was revised to $Cu_3^{2+}Pb^{2+}Te^{6+}O_6(OH)_2$ as a result of their work. As part of our general interest in minerals containing Se and Te (Burns *et al.*, 1995; Hawthorne, 1984; Hawthorne *et al.*, 1986, 1987; Cooper and Hawthorne, 1995, 1996, 2001), we have solved the structure of khinite and present the results here.

Experimental

The sample of khinite used in this work is from the dumps of the Empire mine, Tombstone, Arizona, USA, and was obtained from the mineral collection of the Department of Earth Sciences, Royal Ontario Museum, catalogue number M53319. The crystals have perfect

cleavage parallel to (001) and cleave very easily, producing thin plates (typically <5 μm) that show uniform extinction in cross-polarized light.

Crystal structure

Data collection

A suitable single crystal of khinite was selected for diffraction experiments by examination in plane-polarized and cross-polarized light, attached to a tapered glass fibre and mounted on a Bruker *P*4 diffractometer equipped with a serial detector and graphite-filtered Mo-*K*α X-radiation. Cell dimensions were determined by least-squares refinement of the setting angles of 25 intense reflections and the refined values are given in Table 1. Reflections were measured out to 60º2θ with a fixed scan speed of 0.8º2θ/min and for the following index ranges: $-8 < h < 8$, $0 < k < 14$, $-33 < l < 33$. A total of 1513 reflections were collected over a hemisphere of reciprocal space; further details of the data collection are given in Table 1. Subsequent to the normal data collection, psi-scan data were collected by rotating the crystal about the diffraction vector, psi, and collecting intensities at 6º intervals during complete rotation around psi for ten reflections uniformly spaced between 5 and 60º2θ. The crystal was modelled as a thin (001) plate, and psi-scan correction with a 5º glancing angle reduced $R_{azimuthal}$ from 5.4 to 2.4%. Of the 1321 reflections remaining after standard corrections, 926 are unique and 636 are classed as observed (F_o >4σF). The data were corrected for absorption, Lorentz, polarization and background effects, averaged and reduced to structure factors.

Structure solution and refinement

Scattering curves for neutral atoms were taken from the *International Tables for X-ray Crystallography* (1992). Data merging statistics and systematic absences indicate the space group *Fddd*, as suggested by Williams (1978). The structure was solved by direct methods and converged rapidly to an R_1 index of ~3.5% using alternating difference-Fourier analysis and least-squares refinement (Sheldrick, 1997). However, the resulting structure contained a site that was occupied 50% by Te^{6+} and 50% by Cu^{2+}, with two of the six coordinating O atoms each being split between two very close positions. We regarded this behaviour as crystal-chemically unrealistic, and re-examined the diffraction data. There were no significant observed reflections violating any of the extinction conditions of the space group *Fddd*. Accordingly, we resorted to model building, putting together ordered sheets of Te and Cu octahedra with the right cell-dimensions and then examining the resulting arrangements for the best compatible symmetry. The optimum model had *Fdd*2 symmetry and this was used as a starting structure for least-squares refinement in the space group *Fdd*2. All cations are sited on 2-fold axes parallel to [001] at special positions 8a. There is one Pb site, one Te site and three Cu sites, all fully occupied by their respective cations. Full-matrix least-squares refinement with all cations anisotropic and all anions isotropic converged to R_1 = 3.2%. The absolute structural configuration was clearly established by the Flack parameter of 0.05(2).

TABLE 1. Miscellaneous information for khinite.

a (Å)	5.7491(10)	Crystal size (μm)	$3 \times 60 \times 80$
b (Å)	10.0176(14)	Radiation	Mo-*K*α/Gr
c (Å)	24.022(3)	No. of initial intensities	1513
V (Å^3)	1383.6(4)	**No. of intensities	1321
Space group	*Fdd*2	No. unique	926
Z	8	No. $|F_o| > 4\sigma(|F|)$	636
$D_{meas.}$* (g/cm^3)	6.5−7.0	R_{merge} %	3.5
$D_{calc.}$	6.29	R_1 ($|F_o| > 4\sigma$) %	3.2
		wR_2 (F_o^2) %	7.7
Cell content	$8[Pb^{2+}Cu_3^{2+}Te^{6+}O_6(OH)_2]$		
$R_1 = \Sigma(|F_o|-|F_c|)/\Sigma|F_o|$			
$wR_2 = [\Sigma w(F_o^2- F_c^2)/\Sigma w(F_o^2)^2]^{1/2}$			

* From Williams (1978).
** Total reflections remaining after removal of reflections within 5º glancing angle of the plate.

Inspection of the correlation matrix shows significant correlations between many of the refining parameters, as the majority of the structure is consistent with a centre of symmetry (i.e. *Fddd*). However, convergence was smooth and the final stages of refinement were stable. Final atom parameters are given in Table 2, selected interatomic distances in Table 3 and bond-valences (Brown, 2002) in Table 4.

Description of the structure

Cation sites

There is one Te site which is occupied by Te with a coordination number of [6] and a <Te−O> distance of 1.962 Å. Tellurium may be tetravalent (tellurite) or hexavalent (tellurate) in an oxygen environment. Inspection of <Te−O> distances in tellurite minerals (e.g. emmonsite, Pertlik, 1972; teinite, Effenberger, 1977; magnolite, Grice, 1989; walfordite, Back *et al.*, 1999; winstanleyite, Bindi and Cipriani, 2003) and synthetic compounds (e.g. $TiTe_3O_8$, $SnTe_3O_8$, $HfTe_3O_8$, $ZrTe_3O_8$ (Meunier and Galy, 1971); UTe_3O_9 (Galy and Meunier, 1971); TeO_2 (Leciejewicz, 1961) shows that Te^{4+} is lone-pair stereoactive with three short Te−O distances of ~1.86 Å and a pyramidal coordination, whereas tellurate minerals (e.g. frankhawthorneite, 1.939 Å, Grice and Roberts, 1995; jensenite, 1.936 Å, Grice *et al.*, 1996; leisingite, 1.922 Å, Margison *et al.*, 1997) have Te in octahedral coordination with <Te−O> distances of ~1.93 Å. Thus, Te is hexavalent in khinite. Inspection of Table 4 shows that the incident bond-valence sum at Te is 5.32 valence units (v.u.), significantly less than the ideal value of 6.00 v.u. required by the valence-sum rule (Brown, 1981). This sort of discrepancy is not uncommon in tellurates. Calculation of the incident bond-valence at Te in ten Te-oxysalt compounds: Li_2TeO_4 (5.36 v.u.), Daniel *et al.*, 1977; $CaTeO_4$ (5.51 v.u.), Hottentot and Loopstra, 1979; Na_2TeO_4 (5.56 v.u.), Kratochvil and Jensovsky, 1977; $Na_2Cu_2TeO_6$ (5.61 v.u.), Xu *et al.*, 2005; Ni_3TeO_6 (5.65 v.u.), Becker and Berger, 2006; $Ba_2Nb_2TeO_{10}$ (5.74 v.u.), Mueller-Buschbaum and Wedel, 1996; $CuTeO_4$ (5.72 v.u.), Falck *et al.*, 1978; $SrTe_3O_8$ (5.85 v.u.), Barrier *et al.*, 2006; $Ag_2Te_2O_7$ (5.79, 5.98 v.u.) Klein *et al.*, 2006; and H_2TeO_4 (6.07 v.u.), Moret *et al.*, 1974, shows a range of values from 5.36 v.u. to 6.07 v.u. Stoichiometry forces the valence of Te to be 6+ in all these compounds, and hence the value of 5.32

TABLE 2. Atomic coordinates and displacement parameters for khinite.

	x	y	z	U_{eq}	U_{11}	U_{22}	U_{33}	U_{23}	U_{13}	U_{12}
Pb	¼	¼	0.14110(8)	0.01294(17)	0.0140(3)	0.0100(3)	0.0148(4)	0	0	−0.0009(10)
Te	½	0	0.23761(4)	0.0072(4)	0.0130(9)	0.0007(7)	0.0079(10)	0	0	−0.0018(11)
Cu(1)	0	0	0.29395(17)	0.0082(7)	0.0067(17)	0.0059(15)	0.0119(17)	0	0	−0.0031(18)
Cu(2)	¼	¼	0.29509(13)	0.0052(7)	0.0033(15)	0.0044(15)	0.0079(16)	0	0	−0.0002(16)
Cu(3)	¾	¼	0.23861(17)	0.0089(8)	0.0149(19)	0.0031(14)	0.0088(17)	0	0	−0.0043(17)
O(1)[OH]	0.153(2)	0.1158(14)	0.3466(6)	0.010(3)						
O(2)	0.615(2)	0.1266(14)	0.1834(6)	0.009(3)						
O(3)	0.2002(17)	0.1007(10)	0.2401(4)	0.009(2)						
O(4)	0.6278(18)	0.1221(11)	0.2931(5)	0.012(2)						

TABLE 3. Selected interatomic distances (Å) for khinite.

Pb−O(1)a,b	2.545(14) ×2	Cu(1)−O(1),e	1.928(14) ×2
Pb−O(2),c	2.641(14) ×2	Cu(1)−O(3),e	2.005(10) ×2
Pb−O(3),c	2.823(10) ×2	Cu(1)−O(4)d,f	2.464(11) ×2
Pb−O(4)a,b	2.752(11) ×2	<Cu(1)−O>	2.132
<Pb−O>	2.690		
Te−O(2),d	1.935(14) ×2	Cu(2)−O(1),c	1.912(14) ×2
Te−O(3),d	1.998(10) ×2	Cu(2)−O(3),c	2.017(11) ×2
Te−O(4),d	1.953(11) ×2	Cu(2)−O(4),c	2.523(11) ×2
<Te−O>	1.962	<Cu(2)−O>	2.151
Te−Cu(3)	2.8876(3)	Cu(3)−O(2),g	1.971(14) ×2
Cu(1)−Cu(2)	2.8877(3)	Cu(3)−O(3)c,h	2.990(10) ×2
O(1)···O(2)i	2.660(12)	Cu(3)−O(4),g	1.962(11) ×2
		<Cu(3)−O>	2.308

a: $x-\frac{1}{4}, \bar{y}+\frac{1}{4}, z-\frac{1}{4}$; b: $\bar{x}+, y+\frac{1}{4}, z-\frac{1}{4}$; c: $\bar{x}+\frac{1}{2}, \bar{y}+\frac{1}{2}, z$; d: $\bar{x}+1, \bar{y}, z$; e: $\bar{x}, \bar{y}, z$; f: $x-1, y, z$; g: $\bar{x}+\frac{3}{2}, \bar{y}+\frac{1}{2}, z$; h: $x+1$, y, z; i: $x-\frac{3}{4}, \bar{y}+\frac{1}{4}, z+\frac{1}{4}$

v.u. in khinite is in accord with the hexavalent state of Te in khinite.

There are three Cu sites, all of which are [6]-coordinated and are occupied by Cu with <Cu−Φ> distances (Φ = O, OH) of 2.132, 2.151 and 2.308 Å, respectively. This considerable variation in the <Cu−Φ> values is not particularly unusual. An instability arises as a result of the electronic instability of the d^9 configuration of Cu^{2+} in an octahedral ligand-field, as indicated by the Jahn-Teller theorem (Jahn and Teller, 1937), and there is a spontaneous distortion to a stationary state. Thus $(Cu^{2+}\Phi_6)$ octahedra show four short meridional $Cu^{2+}-\Phi$ distances and two long apical $Cu^{2+}-\Phi$ distances (Burns and Hawthorne, 1995, 1996). As a result of the bond-valence distortion theorem (Brown, 1981, 2002), $<^{[6]}Cu^{2+}\Phi>$ distances increase with increasing distortion of the octahedron away from holosymmetry. This relation has been characterized by Eby and Hawthorne (1993),

with $<^{[6]}Cu^{2+}-\Phi>$ distances varying in the range 2.08−2.35 Å. The values obtained here agree closely with their relation between mean bond length and bond-length distortion from holosymmetry. There is one Pb site occupied by Pb^{2+} and coordinated by eight anions with a <Pb−Φ> distance of 2.690 Å. It is obvious from the bond lengths given in Table 3 that Pb^{2+} is not lone-pair-stereoactive in khinite.

The chemical formula

Williams (1978) wrote the chemical formula of khinite as $PbCu_3TeO_4(OH)_6$, with the same cation ratios and valence assignments as those given here and in Burns *et al.* (1995) for parakhinite. The formula of Williams (1978) differs in its anion constituents, with a total of ten anions and an O:OH ratio of 4:6, as compared with a total of eight anions and an O:OH ratio of 6:2. The chemical composition of Williams (1978) is

TABLE 4. Bond-valence table (v.u.) for khinite.

	Pb	Te	Cu(1)	Cu(2)	Cu(3)	H	
O(1)	0.30 ×2↓		0.51 ×2↓	0.53 ×2↓		0.7	2.04
O(2)	0.24 ×2↓	0.95 ×2↓			0.45 ×2↓	0.3	1.94
O(3)	0.17 ×2↓	0.80 ×2↓	0.41 ×2↓	0.40 ×2↓	0.03 ×2↓		1.81
O(4)	0.19 ×2↓	0.91 ×2↓	0.12 ×2↓	0.10 ×2↓	0.47 ×2↓		1.79
	1.80	5.32	2.08	2.06	1.90	1.0	

compared to the ideal composition derived here from crystal-structure analysis in Table 5. It is apparent that, in addition to the reported impurities of chlorargyrite and quartz, there was also an additional hydrous impurity present. The bond-valence table for khinite (Table 4) shows that the valences Williams (1978) assigned for the cations are correct, whereas the numbers of anions were not: the formula resulting from the structure presented here is $Pb^{2+}Cu_3^{2+}Te^{6+}O_6(OH)_2$.

Bond topology

Both khinite and parakhinite (Burns *et al.*, 1995) contain TeO_6 and $Cu(3)O_6$ octahedra that share *trans* edges to form rutile-like $[MO_4]$ chains that extend parallel to [110] (Fig. 1, layer 1). The $Cu(1)\Phi_6$ and $Cu(2)\Phi_6$ octahedra link similarly to form adjacent parallel $[M\Phi_4]$ chains that share corners with the $[TeCu(3)O_4]$ chains to form an $[M\Phi_2]$ layer of composition $[TeCu_3\Phi_8]$ (Fig. 1,
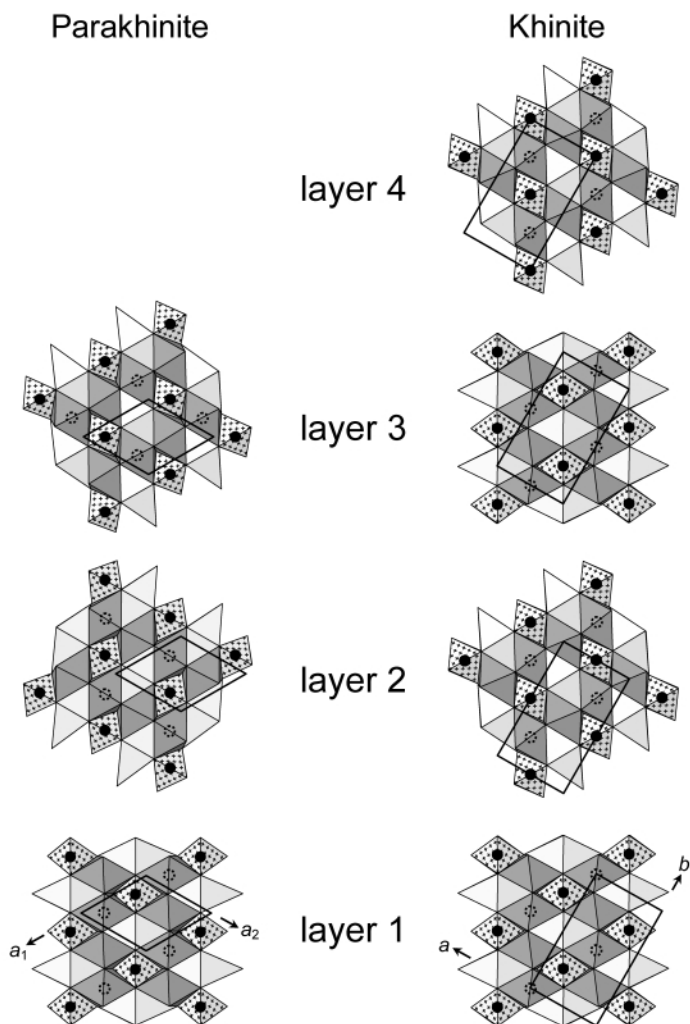

FIG. 1. The $TeCu_3\Phi_8$ layers in parakhinite and khinite projected down [001]. Te polyhedra are shaded light grey with additional small crosses; Cu(3) polyhedra are light-grey; Cu(1) and Cu(2) polyhedra are dark-grey. Pb atoms lying above the layer are filled black circles and dashed circles below the layer. In khinite the Pb atoms lie under the Cu(2) polyhedra, and in parakhinite they lie under the Cu(1) polyhedra. The unit-cell position is outlined in black.

TABLE 5. Khinite and parakhinite chemistry.

	Khinite[1]	Parakhinite[2]	Ideal[3]
CuO	33.2	32.8	36.41
PbO	32.4	31.9	34.05
TeO$_3$	24.5	25.7	26.79
H$_2$O	(7.6)	7.8	2.75
Total	97.7	98.2	100

[1] Williams (1978), H$_2$O by difference.
[2] Williams (1978), H$_2$O by Penfield method.
[3] Calculated from ideal structural formula of khinite/parakhinite.

layer 1). These layers stack along the *c* axis at 6 Å intervals with Pb atoms located between the layers (Fig. 2). In khinite, the [TeCu$_3\Phi_8$] layers are related by 2_1 screw axes along [001] and *d* glide planes parallel to (100) and (010). The successive layers along [001] are shown in Fig. 1 (right) where it can be seen that layers adjacent along *c* are offset laterally relative to adjacent layers. In parakhinite, the [TeCu$_3\Phi_8$] layers are related by a 3_2 screw axis along [001], producing an 18 Å repeat along [001] (Figs 1 and 2) without the lateral offsets that characterize the structure of khinite.

The khinite and parakhinite structures are polar (space groups *Fdd*2 and *P*3$_2$, respectively). This is apparent when viewing the layers 'edge-on' (Fig. 2): the Cu(1) and Cu(2) polyhedra are sited higher than the Te and Cu(3) polyhedra within a given layer, and the interstitial Pb atoms are sited above the Te polyhedra of every layer (Fig. 1). Comparison of the Pb arrangements is shown in Fig. 3, with different shadings used for Pb atoms at different heights along [001]; the Pb[1] atoms lie above layer 1, Pb[2] atoms above layer 2, etc. (see Fig. 2). The positioning of the Pb[1] and Pb[2] atoms is the same in both structures. However, the location of the Pb atoms above layer 3 (i.e. Pb[3]) differs between the two structures. The Pb[4] sites in khinite complete the hexagonal grid pattern of Pb distribution, whereas a 'hole' in the Pb array remains for the parakhinite structure (Fig. 3).

Polytypism

The structures of khinite and parakhinite contain the same layer of polyhedra of composition [TeCu$_3\Phi_8$], and the same linkage between layers is provided by interstitial Pb atoms and H-bonding. It is only the relative stacking of the TeCu$_3\Phi_8$ layers in the *c* direction that distinguishes the two structures (Fig. 1), and hence khinite and parakhinite are polytypes.
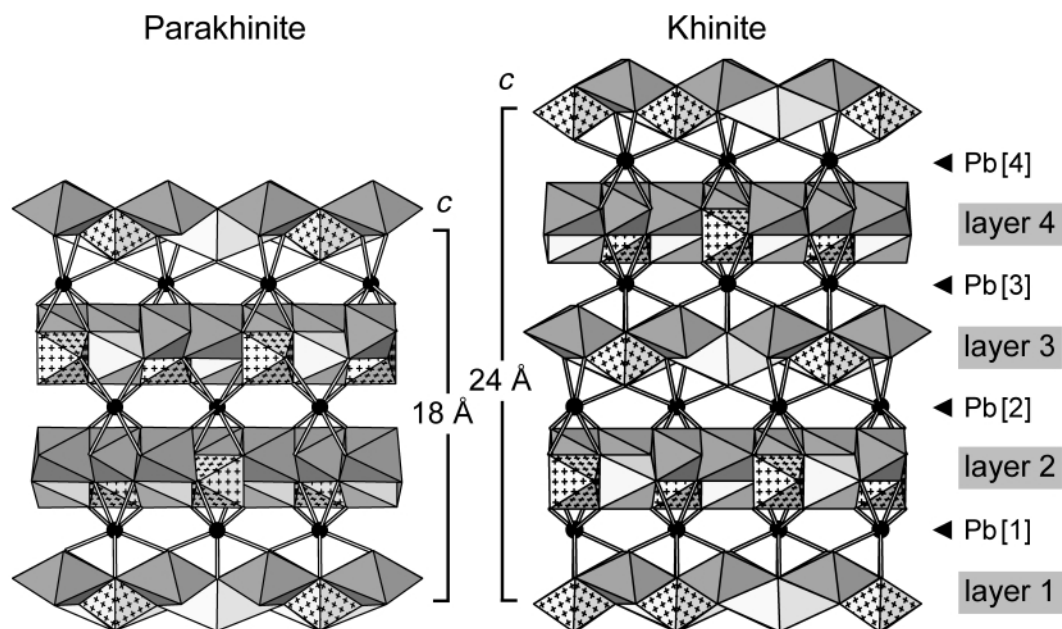

FIG. 2. The structure of parakhinite and khinite projected down [110] and [1$\bar{1}$0], respectively. Legend as in Fig. 1.
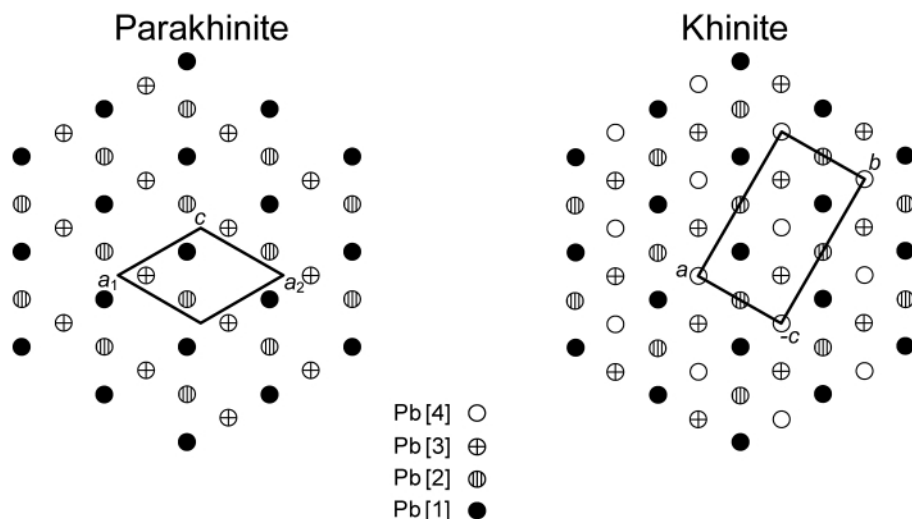
FIG. 3. The pattern of Pb distribution in the structures of parakhinite and khinite projected down [001]. The legend showing the shadings of the Pb atoms Pb[1] → Pb[4] conforms to the labelling of Pb atoms at various elevations along [001] in Fig. 2.

This gross similarity in basic architecture is in accord with the similar calculated densities for the two structures: 6.30 for parakhinite and 6.29 g/cm^3 for khinite.

Acknowledgements

References

Back, M.E., Grice, J.D., Gault, R.A., Criddle, A.J. and Mandarino, J.A. (1999) Walfordite, a new tellurite species from the Wendy open pit mine, El Indio − Tambo mining property, Chile. *The Canadian Mineralogist*, **37**, 1261−1268.

Barrier, N., Malo, S., Hernandez, O., Hervieu, M. and Raveau, B. (2006) The mixed valent tellurate SrTe$_3$O$_8$: Electronic lone pair effect of Te^{4+}. *Journal of Solid State Chemistry*, **179**, 3484−3488.

Becker, R. and Berger, H. (2006) Reinvestigation of Ni$_3$TeO$_6$. *Acta Crystallographica*, **E62**, i222−i223.

Bindi, L. and Cipriani, C. (2003) The crystal structure of winstanleyite, TiTe$_3$O$_8$, from the Grand Central Mine, Tombstone, Arizona. *The Canadian Mineralogist*, **41**, 1469−1473.

Brown, I.D. (1981) The bond-valence method: an empirical approach to chemical structure and bonding. Pp. 1−30 in: *Structure and Bonding in Crystals II* (M. O'Keeffe and A. Navrotsky, editors). Academic Press, New York.

Brown, I.D. (2002) *The Chemical Bond in Inorganic Chemistry. The Bond Valence Model.* Oxford University Press, New York.

Burns, P.C. and Hawthorne, F.C. (1995) Mixed-ligand Cu^{2+}Φ$_6$ octahedra in minerals: observed stereochemistry and Hartree-Fock calculations. *The Canadian Mineralogist*, **33**, 1177−1188.

Burns, P.C. and Hawthorne, F.C. (1996) Static and dynamic Jahn-Teller effects in Cu^{2+} oxysalt minerals. *The Canadian Mineralogist*, **34**, 1089−1105.

Burns, P.C., Cooper, M.A. and Hawthorne, F.C. (1995) Parakhinite, Cu$_3^{2+}$PbTe^{6+}O$_6$(OH)$_2$: crystal structure and revision of the chemical formula. *The Canadian Mineralogist*, **33**, 33−40.

Cooper, M.A. and Hawthorne, F.C. (1995) The crystal structure of guilleminite, a hydrated Ba-U-Se sheet structure. *The Canadian Mineralogist*, **33**, 1103−1109.

Cooper, M.A. and Hawthorne, F.C. (1996) The crystal structure of spiroffite. *The Canadian Mineralogist*, **34**, 821−826.

Cooper, M.A. and Hawthorne, F.C. (2001) Structure topology and hydrogen bonding in marthozite, Cu^{2+}[(UO$_2$)$_3$(SeO$_3$)$_2$O$_2$](H$_2$O)$_8$, a comparison with guilleminite, Ba [(UO$_2$)$_3$ (SeO$_3$)$_2$O$_2$](H$_2$O)$_3$. *The

Canadian Mineralogist, **39**, 797−807.

Daniel, F., Moret, J., Philippot, E. and Maurin, M. (1977) Etude structurale de Li_2TeO_4. Coordination du tellure VI et du lithium par les atomes d'oxygene. *Journal of Solid State Chemistry*, **22**, 113−119.

Eby, R.K. and Hawthorne, F.C. (1993) Structural relations in copper oxysalt minerals. I. Structural hierarchy. *Acta Crystallographica*, **B49**, 28−56.

Effenberger, H. (1977) Verfeinerung der Kristallstruktur von synthetischem Teineit $CuTeO_3(H_2O)_2$. *Tschermaks Mineralogische und Petrographische Mitteilungen*, **24**, 287−298.

Falck, L., Lindqvist, O. and Mark, W. (1978) The crystal structure of $CuTeO_4$. *Acta Crystallographica*, **B34**, 1450−1453.

Galy, J. and Meunier, G. (1971) A propos de la cliffordite UTe_3O_8. Le Système $UO_3−TeO_2$ à 700ºC. Structure crystalline de UTe_3O_9. *Acta Crystallographica*, **B27**, 608−616.

Grice, J.D. (1989) The crystal structure of magnolite, $Hg_2^{1+}Te^{4+}O_3$. *The Canadian Mineralogist*, **27**, 133−136.

Grice, J.D. and Roberts, A.C. (1995) Frankhawthorneite, a unique HCP framework structure of a cupric tellurate. *The Canadian Mineralogist*, **33**, 649−653.

Grice, J.D., Groat, L.A. and Roberts, A.C. (1996) Jensenite, a cupric tellurate framework structure with two coordinations of copper. *The Canadian Mineralogist*, **34**, 55−59.

Hawthorne, F.C. (1984) The crystal structure of mandarinoite, $Fe_2^{3+}Se_3O_9.6H_2O$. *The Canadian Mineralogist*, **22**, 475−480.

Hawthorne, F.C., Ercit, T.S. and Groat, L.A. (1986) Structures of zinc selenite and copper selenite. *Acta Crystallographica*, **C42**, 1285−1287.

Hawthorne, F.C., Groat, L.A. and Ercit, T.S. (1987) Structure of cobalt diselenite. *Acta Crystallographica*, **C43**, 2042−2044.

Hottentot, D. and Loopstra, B.O. (1979) Structures of calcium tellurate, $CaTeO_4$ and strontium tellurate, $SrTeO_4$. *Acta Crystallographica*, **B35**, 728−729.

International Tables for X-ray Crystallography (1992) V.C. Dordrecht, Kluwer Academic Publishers.

Jahn, H.A. and Teller, E. (1937) Stability of polyatomic molecules in degenerate electronic states. I. Orbital degeneracy. *Proceedings of the Royal Society of London A − Mathematical and Physical Sciences*, **A161**, 220−235.

Klein, W., Curda, J., Peters, E.M. and Jansen, M. (2006) $Ag_2Te_2O_7$, ein neues Silbertellurat mit Weberit-Struktur. *Zeitschrift für Anorganische und Allgemeine Chemie*, **632**, 1508−1513.

Kratochvil, B. and Jensovsky, L. (1977) The crystal structure of sodium metatellurate. *Acta Crystallographica*, **B33**, 2596−2598.

Leciejewicz, J. (1961) The crystal structure of tellurium dioxide. *Zeitshcrift für Kristallographie*, **116**, 345.

Margison, S.M., Grice, J.D. and Groat, L.A. (1997) The crystal structure of leisingite, $(Cu^{2+},Mg,Zn)_2$ $(Mg,Fe)Te^{6+}O_6.6H_2O$. *The Canadian Mineralogist*, **35**, 759−763.

Meunier, G. and Galy, J. (1971) Sur une deformation inédite du réseau de type fluorine, structure cristalline des phases MTe_3O_8 (M = Ti, Sn, Hf, Zr). *Acta Crystallographica*, **B27**, 602−607.

Moret, J., Philippot, E., Maurin, M. and Lindqvist, O. (1974) Structure cristalline de l'acide tetraoxotellurique H_2TeO_4. *Acta Crystallographica*, **B30**, 1813−1818.

Mueller-Buschbaum, H. and Wedel, B. (1996) Zur Kenntnis eines Barium-Oxoniobat-Tellurats: $Ba_2Nb_2TeO_{10}$. *Zeitschrift für Naturforschung B − A Journal of Chemical Sciences*, **51**, 1407−1410.

Pertlik, F. (1972) Der Strukturtyp von Emmonsit, $(Fe_2(TeO_3)_3(H_2O(H_2O)_x$ (x = 0−1). *Tschermaks Mineralogische und Petrographische Mitteilungen*, **18**, 157−168.

Sheldrick, G.M. (1997) *SHELX−97: Program for the solution and refinement of crystal structures*. Siemens Energy and Automation, Madison, WI, USA.

Williams, S.A. (1978) Khinite, parakhinite, and dugganite, three new tellurates from Tombstone, Arizona. *American Mineralogist*, **63**, 1016−1019.

Xu, J., Assoud, A., Soheilnia, N., Derakhshan, S., Cuthbert, H.L., Greedan, J.E., Whangbo, M.-H. and Kleinke, H. (2005) Synthesis, structure, and magnetic properties of the layered copper(II) oxide $Na_2Cu_2TeO_6$. *Inorganic Chemistry*, **44**, 5042−5046.